

Original Article

Highly Regulative DC Power Supply Units for Space Applications using Spacecrafts Standard Power Buses

Sunanda¹, Supreeth², Bhanuprakash³, Adinath⁴

^{1,2,4}EEE, RV College of Engineering, Karnataka, India.

³Power Design, Centum Electronics Limited, Karnataka, India.

¹Corrsponding Author : sunandac@rvce.edu.in

Received: 09 November 2025

Revised: 11 December 2025

Accepted: 10 January 2026

Published: 14 January 2026

Abstract - The research paper focuses on the design and hardware implementation of a one-switch DC to DC forward converter topology with a coupled inductor as a post regulator to provide dual outputs of 5V and 3.3V. The input is in the range of 65 to 75volts, commonly available from spacecraft's standard power buses. Voltage feed-forward control method is employed, and the proposed topology is optimized for space applications, offering improved line and load regulations, and reduced ripples in outputs. The novelty in the research work is the use of coupled inductors as post regulators and nanocrystalline ferrite cores for transformers. A nanocrystalline ferrite core transformer is used to reduce heating and core losses. By employing coupled inductors, the design achieves better magnetic coupling and minimizes leakage inductance. The resulting converter architecture meets the performance and safety requirements of space constraints. The experimental results obtained from the hardware prototype are presented to validate the performance of the designed converter. Across all load conditions, the line and load regulations of the designed converter remain below 1%. The proposed forward converter uses the solar energy stored in the spacecrafts power buses and converts it into constant 5V & 3.3V DC values to power the digital devices present in the spacecrafts.

Keywords - Forward converter, Coupled inductor, Leakage inductance, Voltage ripple, Line regulation, Load regulation.

1. Introduction

Spacecraft typically use power buses with voltages of 28V, 50V, or 65V, often supplied by solar arrays or battery systems. Solar panels are the primary energy source for most satellites, and many newer spacecraft designs adopt a 65V power bus because it allows for more efficient power transmission by reducing current draw and the need for thicker cables. In cases where solar power is insufficient, lithium-ion batteries charge up to 65V and provide the necessary backup power.

This readily available 65V input is then stepped down to 5V and 3.3V to power various onboard digital devices such as processors, memory devices, FPGAs, and sensors. These components require stable, highly regulated voltages, often at 3.3V or 5V, due to their sensitivity to voltage fluctuations. However, a key challenge in space power systems is maintaining precise voltage regulation under varying load conditions, especially when multiple outputs are required. The existing DC-to-DC converters face issues with line and load regulation, as well as cross-regulation between dual outputs, particularly in single-switch forward converter designs [1-13].

In high-performance systems like spacecraft, even small fluctuations in voltage can compromise the functionality of

sensitive electronic components. This is the research gap that this work addresses: improving the line and load regulation and reducing the cross-regulation between multiple outputs in a single-switch forward converter [14-16].

One promising approach to addressing these issues is the use of coupled inductors as post-regulators. By tightly coupling the inductors for the different outputs on a single core, leakage inductance is minimized, and voltage regulation can be significantly improved. This design aims to enhance the coupling between the inductors, thereby reducing the ripple and cross-regulation between the outputs [15-24].

The main objective of this research is to design and implement a single-switch forward converter using coupled inductors as post-regulators to address the limitations in voltage regulation for dual outputs.

1.1. Literature Review

The voltage feed-forward control technique has a faster response. It provides better line regulation than the case of the voltage feedback control method. Magnetic amplifiers and low-dropout regulators regulate each output in multiple-output forward converters, thus improving load regulation. [1] Shweta et al. (2021) in [2] proved that the voltage feedback



control method is slower than the voltage feed-forward control. Maksimovic et al. (2000) in [3] compared coupling methods: near-ideal coupling, practical moderate coupling, and the zero-ripple approach for coupled inductors. The zero-ripple method showed better cross-regulation results. .

Zhu Feiyang et al. (2021) in [4] compared the performance of coupled inductors and non-coupled inductors with respect to different applications. Coupled inductors showed better performance. Juan R et al. (2023) in [5] proved that low output voltage ripples are achieved by using switched-capacitor blocks in forward converters for high step-down requirements.

Zhou G et al. (2022) in [6] proposed a three-port forward converter with a small structure. The range of duty cycle was also extended. It has one extra diode and switch when compared with the traditional two-switch forward converter. T Siwakorn et al. (2023) in [7] presented a buck converter design to directly power sensitive analog circuits used in low-power System-On-Chips (SoCs). Without the help of Low-Dropout voltage regulators (LDOs), low voltage ripples were obtained by the employment of a Pulse-Frequency Modulation (PFM) scheme.

Yan Lu et al. (2021) in [8] presented a two-phase three-level buck converter. Its speciality was that it had Cross-Connected Flying capacitors (X-CFLY). The inductor currents, which were unbalanced, were suppressed in the two-phase operation of the converter. A small output ripple and faster transient response were achieved by this technique. Meyers Marc A et al. (2006) in [9] detailed the important mechanical properties of nanocrystalline materials. Allahyari H et al. (2023) in [10] proposed a single switch forward converter which was controlled with variable magnetizing inductance. It provided synchronous rectification, which was self-driven. A wide range of ZVS conditions is obtained using an auxiliary capacitor alongside leakage and magnetizing inductances.

Suryanarayana C et al. (2000) in [11] discussed the synthesis, structure, thermal stability, and properties of nanocrystalline materials. Hemalatha J N et al. (2019) in [12] proved that the converter fed with unsynchronized PWM pulses gives lower efficiency than the converter fed with synchronized pulses. Qiang Li et al. (2022) in [13] compared an indirect-coupled inductor (ICL) with a non-coupled inductor as output regulators for a multi-phase buck converter.

Nagesh L et al. (2020) in [14] designed power supply units for space applications. For this, a triple-output forward converter was used. Reduced output voltage ripples were observed by using coupled inductors as post-output regulators. Rampelli et al. (2012) in [15] aimed to design a Forward Converter Topology operating at resonant reset mode with a fixed high frequency. Power loss is eliminated in the reset

circuit by using the self-resonant reset method. L Jennifer et al. (2018) in [16] implemented over-temperature, over-current, and over-voltage protection circuits for DC-DC converters and analysed their performance. V Chippalkatti et al. (2016) in [17] aimed at designing a voltage feed-forward controlled multiple-output forward converter. A magnetic amplifier (Mag-amp) was used as a post regulator. Mag-amp provides good load regulation by regulating the output from any load changes.

Dharmraj V et al. (2002) in [18] presented a dual two-transistor modelled forward converter with both zero voltage and current switching schemes. The two Similar Two-Transistor Forward Converters (TTFC) are coupled through a single transformer and are also connected in series. It is suitable for high-power and high input voltage applications as it operates in a full bridge mode. Kefas D et al. (2003) in [19] presented a new four-switch converter. It can be used especially in low-power applications and high-input-voltage applications. Same gate pulses are given to all four switches, but internal switches are turned on after some small delay time during the off time of the internal switches, preventing a direct short circuit in the DC link. This positioning, thus, makes the converter very useful for auxiliary power supplies.

Sunil K et al. (2024) in [20] designed a non-cascading structure for a flyback-forward converter to increase the range of the duty cycle, beyond 50%. Suresh K et al. (2022) in [21] proposed a forward converter SMPS with low noise operated at high frequency. To reduce the size, weight, noise, and switching losses, a high-frequency switching technique is used.

S Patil et al. (2020) in [22] designed a technique called active clamp reset for forward converters. In a normal forward converter, this technique is used to reset the power transformer. Using this technique, a duty cycle of greater than 50% was achieved. Hariprasad S A et al. (2015) in [23] presented a dual-input SEPIC converter. The dual-input SEPIC converter can be used for power supplies instead of using two single converters.

1.2. Overview

The proposed research work used a single-switch dual-output forward converter with coupled inductors as post-regulators, unlike most prior works [1, 2, 14, 15, 17, 22], which used multi-output forward converters with Mag-amp or LDO post-regulators. Nanocrystalline ferrite cores are used for transformers and inductors, unlike most designs [1, 2, 14, 17], which use ferrite cores. The designed converter operates at 200 kHz, while [15, 21, 22] were operated at a typical range of 100–150 kHz. The proposed work provided a hardware implementation of a coupled inductor as a post-regulator in a dual-output forward converter, while [3, 4, 13] focused on modelling and analysis of coupled inductors in multi-phase regulators, not experimental realization in forward converters.

The work presented in this paper is designed for 65–75V input, matching spacecraft power buses, while most papers [1, 2, 14] are designed for terrestrial or industrial 28V or 48V buses.

[1, 14, 17], typical reported values <3% and not always experimentally validated under dual-load. [1, 14, 17] targeted space applications but used bulkier multi-switch systems. Many works [2, 6, 13, 20] are limited to only simulations. Many works [10, 17, 21] showed efficiencies of around 70–75%. The proposed research work experimentally validated a <1% line and load regulation under all conditions and achieved up to 76.9% efficiency at 50% load. It was also optimized for size, weight, and thermal efficiency, especially for space applications.

Considering all previous research papers. Transformers made of nano-crystalline materials are found to have less heating losses and core losses. Voltage feed-forward control is found to be good for reduced line regulation. A coupled inductor as a post regulator for dual outputs is found to be good for reduced load and cross-regulations. Hence, combining all these features in one project and also utilizing the saved solar energy in the spacecrafts can make this research work a novel one.

2. Functional Block Diagram

Figure 1 shows the detailed diagram of the designed forward-converter in terms of blocks. The designed forward-converter is used to step down input voltages in the range of 65–75 volts to 2 different regulated output voltages, 5 and 3.3 volts. 5V output is regulated for a fixed full load current of 10.8A, and 3.3V output is regulated for a fixed full load current of 2.7A.

The designed forward-converter is able to generate an output power of 63 watts. The designed forward-converter is designed for overcurrent protection and under-voltage protection. Voltage feedback control is implemented for the closed-loop operation of the designed converter. The original output voltage and the reference voltage are compared in order to generate an error signal.

Based on the error signals generated, the duty cycle of the MOSFET switch is varied. THE PWM IC UC2825 is used to generate gate pulses. An optocoupler is used for isolation of the output side feedback circuit and the input side PWM IC. The differential and common mode filters are used to reduce noise and electromagnetic interference of the raw input voltage.

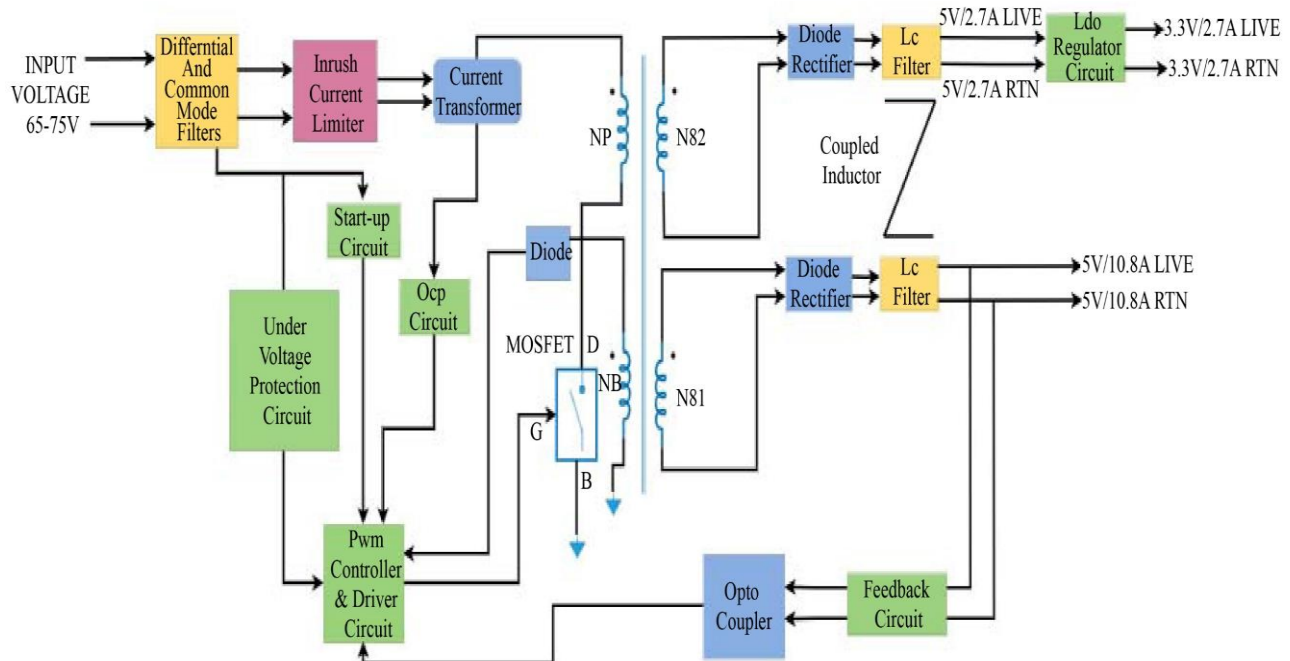


Fig. 1 Block diagram of the designed converter

Figure 2 shows the equivalent circuit diagram of the designed forward-converter. An inrush current limiter circuit is designed to reduce the large surge of current that occurs when the converter is first turned on, protecting components from damage. The two secondary windings of the transformer

have the same number of turns. The output across the first secondary winding is 5V/10.8A. The output across the second secondary winding is 5V/2.7A. The Low dropout regulator is used as a post regulator to convert 5V/2.7A to 3.3V/2.7A.

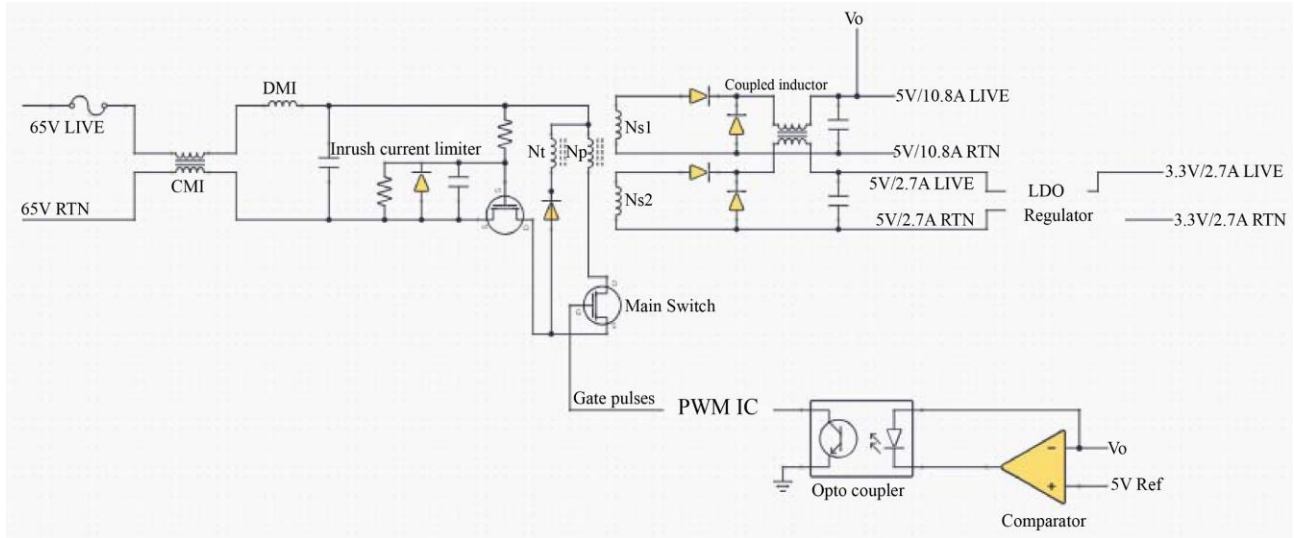


Fig. 2 Circuit diagram of the designed converter

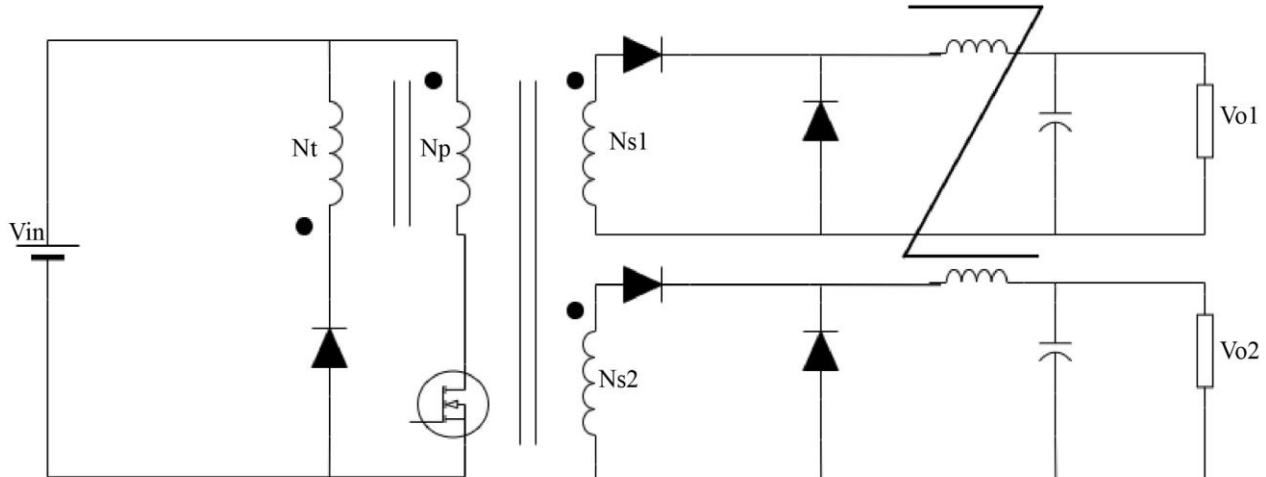


Fig. 3 Coupled inductor topology

2.1. Coupled Inductor Topology

A coupled inductor topology in a single switch dual output forward converter is shown in Figure 3. A coupled inductor is created by tightly coupling individual filter inductors of the two outputs in a single core. The forward converter-coupled inductor topology offers improved coupling and reduced leakage inductance, thereby increasing the overall efficiency of the forward converter. The coupled inductor itself facilitates voltage regulation by reducing both load and cross-regulation of the output voltages.

2.2. Working Principle of the Designed Converter

The designed forward-converter has two modes of operation. Figure 4 shows the operation of the designed forward-converter using a start-up circuit. Initially, when the converter is turned on, the bias circuit requires some microseconds to operate and produce a voltage to turn on the PWM IC. So, the start circuit will operate in that period and

produce 10.5V to turn on the PWM IC. Figure 5 shows the operation of the designed forward-converter using a bias circuit. Once the bias circuit starts to operate, it produces a voltage of 12V, which is now used to power the PWM IC. So, the start circuit is no longer required to power the PWM IC.

3. Specifications and Design Details

Minimum Input voltage, $V_{in(min)} = 60V$

Maximum Input voltage, $V_{in(max)} = 80V$

Switching Frequency, $F_{sw} = 200$ kHz

$D_{max} = 0.4$

$$D_{min} = \frac{(D_{max} * V_{in(min)})}{V_{in(max)}} \quad (1)$$

Efficiency, $Eff = 0.75$

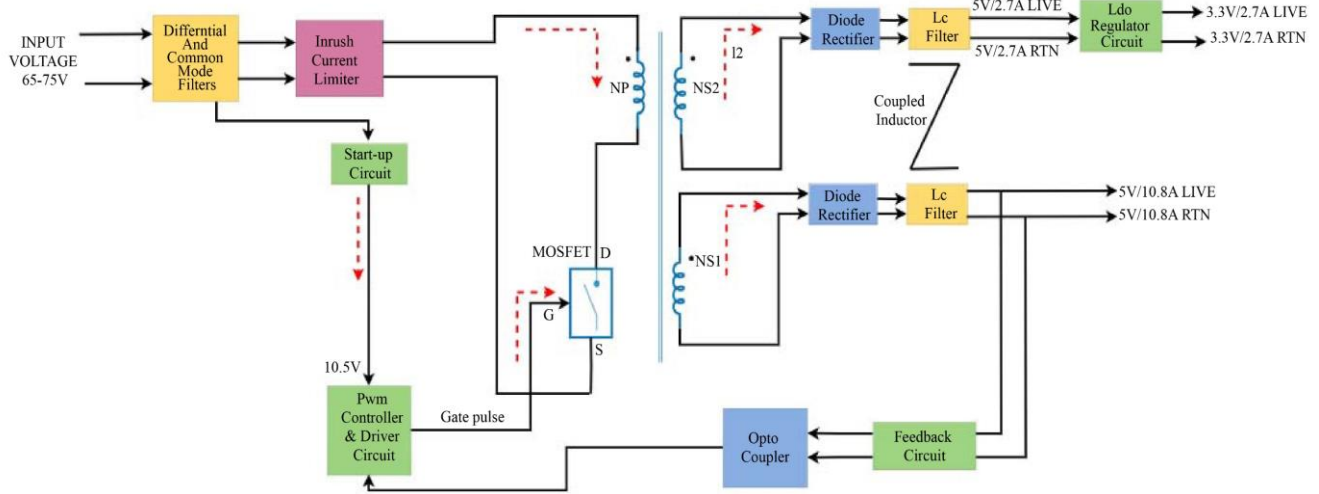


Fig. 4 Operation using the startup circuit

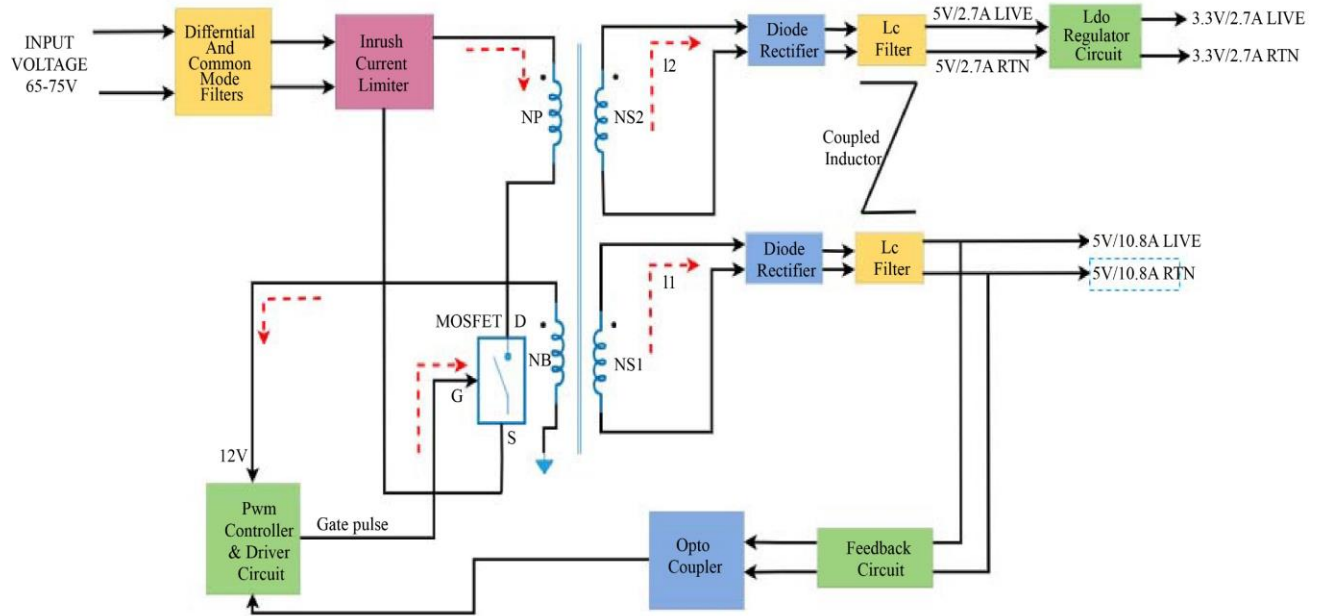


Fig. 5 Operation using bias circuit

Equation (1) is used to find the minimum value of the duty cycle. Design is done to achieve higher efficiency. Switching frequency is chosen as 200KHz, considering switching losses, mass, size of filters, and transformer design. The design specification of the proposed Forward Converter is as given in Table 1.

Table 1 shows the forward converter specifications with respect to different factors like input voltage, output voltage, power rating, switching frequency, etc. According to the forward converter specifications, the values of the inductor and capacitors are calculated.

Table 1. Title of the table

Converter Specification Details	
Parameters	Specification
Input voltage	65-75V DC
Output voltage	5V & 3.3V DC
Output Current	10.8A & 2.7A
Switching Frequency	200 kHz
Line Regulation	<1%
Load Regulation	<1%

3.1. Transformer Design

$$D_{\max} = 0.4$$

$$Eff = 0.75$$

$$K_w = 0.4$$

$$J = 4 \text{ Amp/mm}^2$$

$$B_m = 0.08 \text{ tesla}$$

Normally, Window Factor (Kw) can vary from 0.3 to 0.5. Flux Density (Bm) depends on core material, and it can vary from 0.121 to 0.199 for ferrite cores. Current Density (J) can vary from 3A/mm² to 6A/mm².

$$Ap = \frac{\sqrt{D_{\max}} * (P_{out}(1 + 1/eff) * 10^6)}{K_w * J * B_m * F_{sw}} \quad (2)$$

Nanocrystalline ferrite material is used as the core for a transformer. Nanocrystalline ferrite core is used to reduce heating and core losses. Equation (2) shows the equation for the calculation of the area product. The total transformer power loss of transformers made of nanocrystalline ferrite material is 1.28 watts. Whereas, the total transformer power loss of transformers made of ferrite material is 3.96 watts. The power losses of nanocrystalline ferrite transformers are much lower compared to traditional transformers. This is one of the novelties of the research work.

3.2. Turns Ratio

Equation (3) shows the equation for the calculation of the turn's ratio.

$$Tratio = \frac{V_{out} + (V_D * D_{\max})}{D_{\max} * V_{in(min)}} \quad (3)$$

Therefore,

$$T_{ratio1} = 0.2225$$

$$T_{ratio2} = 0.2175$$

$$T_{ratio, bias} = 0.5108$$

3.3. Selection of the Number of Turns

$$N_p = \frac{V_{in(min)} * D_{\max}}{B_m * A_c * 10^{-6} * F_{sw}} \quad (4)$$

Equation (4) shows the equation for the calculation of the number of turns of the primary winding. Therefore, Np is taken as 64 turns. Using Equations (5), (6), and (7), the number of turns of 2 secondary windings and one bias winding can be calculated,

$$Ns1 = N_p * Tratio1 = 14.24 \quad (5)$$

$$Ns2 = N_p * Tratio2 = 13.92 \quad (6)$$

$$Nbias = N_p * Tratio_bias = 32.6933 \quad (7)$$

3.4. Output 1 Filter Design

Given,

$$D_{\min} = 0.3$$

$$D_{min1} = 0.8 * D_{min} = 0.24 \quad (8)$$

$$V_{out1} = 5V$$

$$I_{out1} = 10.8A$$

$$K_1 = 0.2$$

$$L1 = \frac{V_{out1} * T_s * (1 - D_{min1})}{2 * K_1 * I_{out1}} \quad (9)$$

Therefore, L1 = 4.3981uH.

Equation (8) is used to find the minimum duty cycle for output 1. Its value is 0.24. Equation (9) is used to find the minimum inductance value for output 1. Equation (10) is used to find the minimum capacitance value for output 1.

Given,

$$\Delta V_1 = 0.025$$

$$F_{sw} = 200\text{khz}$$

$$C_1 = \frac{K_1 * I_{out1}}{8 * F_{sw} * \Delta V_1} \quad (10)$$

Therefore, C1 = 54uF.

3.5. Output 2 Filter Design

Given,

$$D_{\min} = 0.3$$

$$D_{min1} = 0.8 * D_{min} = 0.24 \quad (11)$$

$$V_{out2} = 5V$$

$$I_{out2} = 2.7A$$

$$K_2 = 0.6$$

$$L2 = \frac{V_{out2} * T_s * (1 - D_{min2})}{2 * K_2 * I_{out2}} \quad (12)$$

Therefore, L2 = 5.8642uH.

Equation (11) is used to find the minimum duty cycle for output 2. Its value is 0.24. Equation (12) is used to find the minimum inductance value for output 2. Equation (13) is used to find the minimum capacitance value for output 2.

Given,
 $\Delta V_2 = 0.015$

$f_{sw} = 200\text{kHz}$

$$C_2 = \frac{K_2 * I_{out2}}{8 * f_{sw} * \Delta V_2} \quad (13)$$

Therefore, $C_2 = 67.5\text{uF}$.

3.6. Hardware Implementation



Fig. 6 Hardware setup of the designed converter

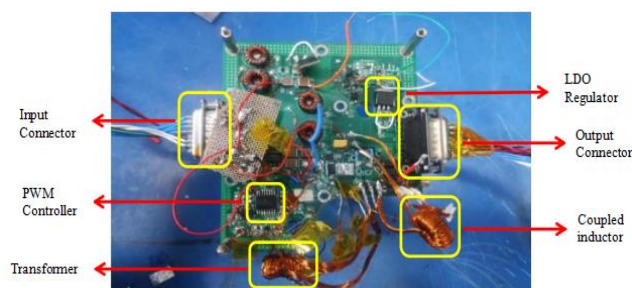


Fig. 7 Top view of the designed converter

Figure 6 shows the picture of the experimental setup of the designed converter. Input Voltage to the forward converter is in the range of 65–75 VDC and is given via the K1 connector. To turn on and off the forward converter, an ON/OFF command control telemetry is used. The ON/OFF command control telemetry is powered by a 5V power supply. Figure 7 shows the image of the designed forward-converter in PCB when viewed from the top.

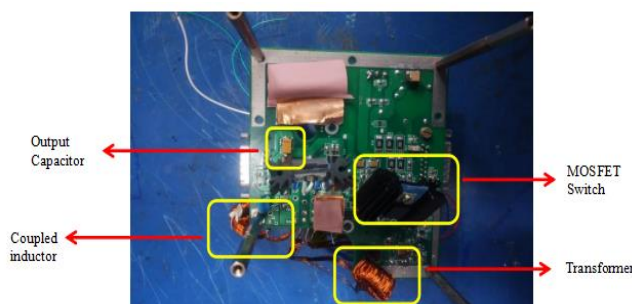


Fig. 8 Bottom view of the designed converter

Figure 8 shows the image of the designed forward-converter in PCB when viewed from the bottom. The experimental results for two outputs are individually tabulated and are shown in the tables below.

4. Results and Discussion

4.1. Output Voltage Results

Table 2. Dual output voltage 1 results

Vin (V)	OUTPUT VOLTAGE (V)		
	10% load	50% load	100% load
65.00	5.008	5.011	5.013
70.00	5.009	5.010	5.013
75.00	5.009	5.010	5.013

Table 2 shows the dual output voltage 1 results of the designed forward-converter for 3 input voltages, 65, 70, and 75V, against 3 different loads, 10, 50, and 100%. Table 3 shows the dual output voltage results of the designed forward-converter for 3 input voltages, 65, 70, and 75V, against 3 different loads, 10, 50, and 100%.

Table 3. Dual output voltage 2 results

Vin (V)	OUTPUT VOLTAGE (V)		
	10% load	50% load	100% load
65.00	3.310	3.307	3.304
70.00	3.310	3.308	3.305
75.00	3.310	3.307	3.304

Table 4 shows the input power results of the designed forward-converter for 3 input voltages, 65, 70, and 75V, against three different loads, 10, 50, and 100%.

Table 4. Input power results

Vin (V)	INPUT POWER (W)		
	10% load	50% load	100% load
65.00	9.945	40.95	83.655
70.00	9.918	41.58	83.790
75.00	10.125	41.85	83.700

4.2. Power Results

Table 5 shows the output power results of the designed forward-converter for three input voltages, 65, 70, and 75V, against 3 different loads, 10, 50, and 100%.

Table 5. Output power results

Vin (V)	OUTPUT POWER (W)		
	10% load	50% load	100% load
65.00	6.3061	31.530	63.034
70.00	6.3047	31.518	63.369
75.00	6.3023	31.517	63.061

4.3. Line Regulation Results

Table 6. Line regulation 1 results

Vin (V)	Line Regulation (%)		
	10% load	50% load	100% load
65V - 70V	0.02	0.02	0
70V - 75V	0	0	0

Table 6 shows the line regulation 1 results of the designed forward-converter for 3 input voltages, 65, 70, and 75V, against three different loads, 10, 50, and 100%.

Table 7. Line regulation 2 results

Vin (V)	Line Regulation (%)		
	10% load	50% load	100% load
65V - 70V	0	0.02	0.02
70V - 75V	0	0.02	0.02

Table 7 shows the line regulation 2 results of the designed forward-converter for 3 input voltages, 65, 70, and 75V, against 3 different loads, 10, 50, and 100%.

4.4. Load Regulation Results

Table 8. Load regulation 1 results

Vin (V)	Load Regulation (%)		
	10% load	50% load	100% load
65.00	0.16	0.22	0.26
70.00	0.18	0.20	0.26
75.00	0.18	0.20	0.26

Table 8 shows the load regulation 1 results of the designed forward-converter for 3 input voltages, 65, 70, and 75V, against 3 different loads, 10, 50, and 100%. Table 9 shows the load regulation 2 results of the designed forward-converter for 3 input voltages, 65, 70, and 75V, against 3 different loads, 10, 50, and 100%

Table 9. Load regulation 2 results

Vin (V)	Load Regulation (%)		
	10% load	50% load	100% load
65.00	1	0.7	0.4
70.00	1	0.8	0.5
75.00	1	0.7	0.4

4.5. Efficiency Results

Table 10 shows the efficiency results of the designed forward-converter for 3 input voltages, 65, 70, and 75V, against 3 different loads, 10, 50, and 100%. It is observed from the efficiency results table that efficiency is maximum for an input voltage of 65 volts out of the 3 input voltages. Also, it is observed from the efficiency results table that efficiency is maximum for 50% load out of the 3 loads.

Table 10. Efficiency results

Vin (V)	EFFICIENCY (%)		
	10% load	50% load	100% load
65.00	63.4	76.9	75.3
70.00	63.5	75.8	75.6
75.00	62.2	75.3	75.3

4.6. Waveforms

Figures 9 and 10 show the dual output 1 and dual output 2 voltage waveform of the designed forward-converter for 100% load. It is observed from the waveforms that the output voltage is a constant DC.

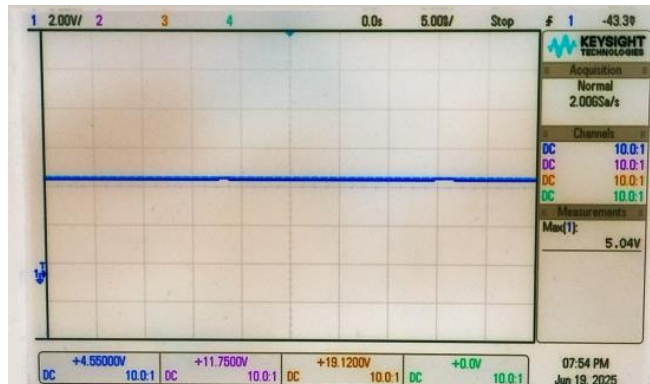


Fig. 9 Dual output 1-voltage waveform

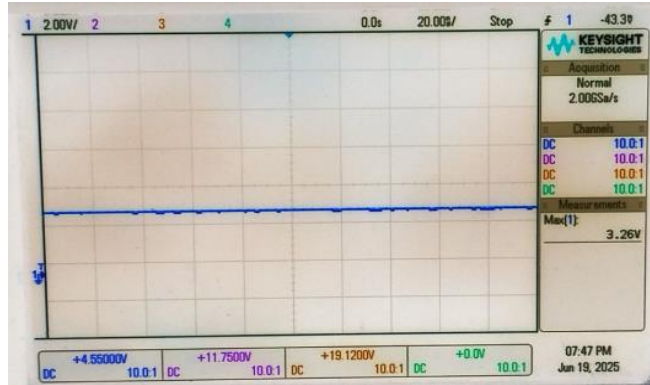


Fig. 10 Dual-output 2-voltage waveform

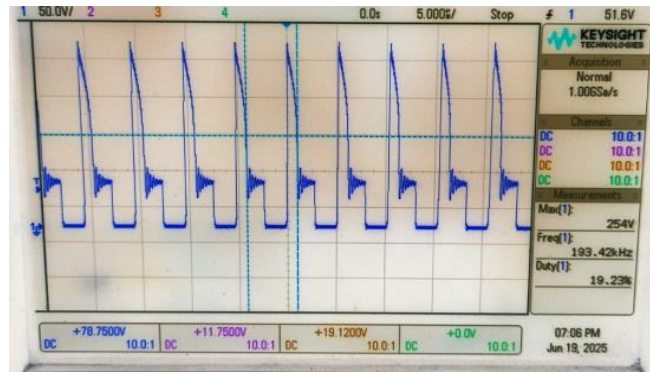


Fig. 11 Vds waveform

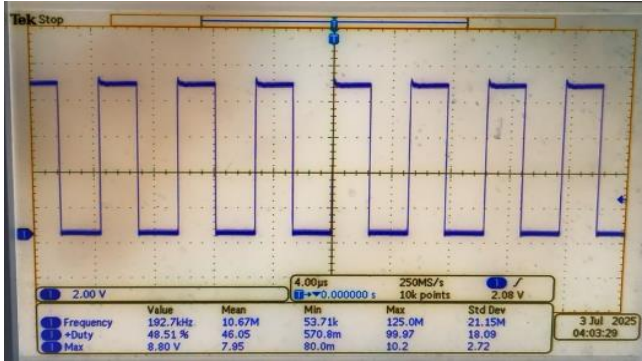


Fig. 12 Vgs waveform

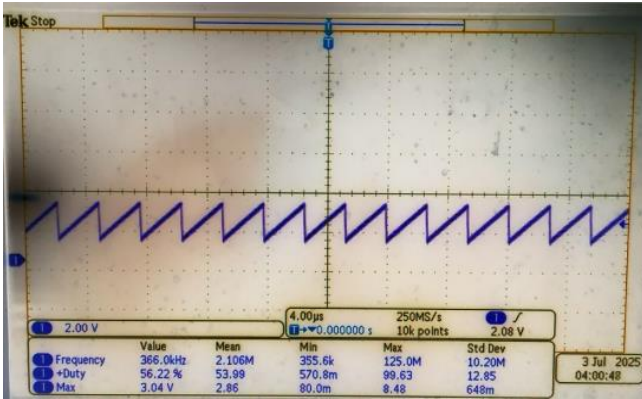


Fig. 13 Ramp waveform

Figures 11 and 12 show the V_{ds} and V_{gs} waveforms of the designed converter for 100% load. Figure 13 shows the ramp waveform of the PWM IC. The proposed design achieves line and load regulation below 1% for both outputs under all load conditions, which is significantly better than many traditional multi-output converter designs that typically struggle with cross-regulation and precise voltage control, especially when loads fluctuate. The use of coupled inductors as post-regulators ensures tighter magnetic coupling, which further reduces voltage ripple and cross-regulation problems often observed in conventional designs. The adoption of nanocrystalline ferrite cores for both transformers and inductors in the design is a clear improvement over conventional ferrite cores. This choice results in reduced heating and lower core losses. It is observed from the results that nanocrystalline cores exhibit 1/2 to 1/5 the losses of standard ferrite materials. The converter designed in the research work is matched to the 65V power bus standard found in modern spacecraft and is optimized to supply both 5V and 3.3V high-stability rails for digital payloads. It is a crucial

requirement for new-generation satellites that rely on sensitive semiconductor devices. Most prior studies stayed below 48V or only simulated performance. The research proposed a unique integration of voltage feed-forward control (for fast and stable response), coupled inductors (minimized leakage inductance and ripple), nanocrystalline magnetic materials (highest efficiency and lowest losses), and utilizing the stored energy in spacecrafts to power digital devices, unlike many prior works that use individual improvements separately. No prior work has combined all these features in one system. Experimental data demonstrates that peak efficiency reaches up to 76.9% at 50% load, which is a notable achievement for this class of converters. Prior references suggest typical efficiencies lower than this for similar dual-output designs under comparable conditions. The complete hardware demonstration, including testing across multiple load cases, experimentally verifies the effectiveness of the design, moving it a step beyond most existing research that is often simulation-based or only partially validated in hardware. Unlike previous multi-output forward converters that rely on magnetic amplifiers or LDO regulators [1, 14, 17], the proposed design integrates coupled inductors as passive post-regulators, significantly minimizing cross-regulation and voltage ripple. Furthermore, the adoption of nanocrystalline ferrite transformer cores reduces magnetic losses by 68%, while the single-switch feed-forward control scheme ensures line and load regulation below 1% across the 65–75 V input range, making the design uniquely optimized for spacecraft power systems. These points collectively demonstrate that the research work is not only technically novel but also more suitable for demanding real-world applications, such as space power management, thereby setting it apart from previously reported solutions.

5. Conclusion

The converter was designed and implemented as a hardware PCB prototype. For all load conditions, the designed converter has line and load regulations below 1%. The dual outputs 5V and 3.3V were achieved for an input range of 65–75 volts. The dual outputs were highly regulative in nature with very few ripples. Hence, the designed converter can be used in space applications to step down the 65V standard bus voltage to 5V and 3.3V, respectively, to provide a supply to various digital devices.

Funding Statement

The research and publication of the article are funded by RV College of Engineering.

References

- [1] Soumya Patil et al., "Design and Implementation of Multiple Output Forward Converter with Mag-Amp and LDO as Post Regulators for Space Application," *International Journal of Engineering, Science and Technology*, vol. 12, no. 3, pp. 43-56, 2020. [[CrossRef](#)] [[Google Scholar](#)] [[Publisher Link](#)]
- [2] S.P. Shweta, B.K. Singh, and Rudranna Nandihalli, "Dual Output Forward Converter with Feed Forward Control for Space Applications," *International Research Journal of Engineering and Technology (IRJET)*, vol. 8, no. 6, pp. 887-892, 2021. [[Google Scholar](#)] [[Publisher Link](#)]

- [3] Dragan Maksimović, Robert W. Erickson, and Carl Griesbach, "Modeling of Cross-Regulation in Converters Containing Coupled Inductors," *IEEE Transactions on Power Electronics*, vol. 15, no. 4, pp. 607-615, 2000. [[CrossRef](#)] [[Google Scholar](#)] [[Publisher Link](#)]
- [4] Feiyang Zhu, Qiang Li, and Fred C. Lee, "Modeling and Analysis of Multi-Phase Coupled Inductor Structures for Voltage Regulators," *2021 IEEE Energy Conversion Congress and Exposition (ECCE)*, Vancouver, BC, Canada, pp. 5507-5514, 2021. [[CrossRef](#)] [[Google Scholar](#)] [[Publisher Link](#)]
- [5] Juan Rodríguez et al., "High Step-Down Isolated PWM DC-DC Converter based on Combining a Forward Converter with the Series-Capacitor Structure," *IEEE Access*, vol. 11, pp. 131045-131063, 2023. [[CrossRef](#)] [[Google Scholar](#)] [[Publisher Link](#)]
- [6] Guohua Zhou, Qingxin Tian, and Haoze Li, "Three-Port Forward Converters with Compact Structure and Extended Duty Cycle Range," *IEEE Transactions on Industrial Electronics*, vol. 70, no. 1, pp. 566-581, 2023. [[CrossRef](#)] [[Google Scholar](#)] [[Publisher Link](#)]
- [7] Siwakorn Thongmark, and Woradorn Wattanapanitch, "Design of a High-Efficiency Low-Ripple Buck Converter for Low-Power System-On-Chips," *IEEE Access*, vol. 11, pp. 122566-122585, 2023. [[CrossRef](#)] [[Google Scholar](#)] [[Publisher Link](#)]
- [8] Chuang Wang et al., "A Two-Phase Three-Level Buck Converter with Cross-Connected Flying Capacitors for Inductor Current Balancing," *IEEE Transactions on Power Electronics*, vol. 36, no. 12, pp. 13855-13866, 2021. [[CrossRef](#)] [[Google Scholar](#)] [[Publisher Link](#)]
- [9] Marc André Meyers, Anuj Mishra, and David J. Benson, "Mechanical Properties of Nanocrystalline Materials," *Progress in Materials Science*, vol. 51, no. 4, pp. 427-556, 2006. [[CrossRef](#)] [[Google Scholar](#)] [[Publisher Link](#)]
- [10] Hesamodin Allahyari et al., "An Improved Single Switch Wide Range ZVS Forward Converter Controlled with Variable Magnetizing Inductance," *IEEE Journal of Emerging and Selected Topics in Industrial Electronics*, vol. 5, no. 3, pp. 837-847, 2024. [[CrossRef](#)] [[Google Scholar](#)] [[Publisher Link](#)]
- [11] C. Suryanarayana, and C.C. Koch, "Nanocrystalline Materials-Current Research and Future Directions," *Hyperfine Interactions*, vol. 130, no. 1-4, pp. 5-44, 2000. [[CrossRef](#)] [[Google Scholar](#)] [[Publisher Link](#)]
- [12] J.N. Hemalatha, S.A. Hariprasad, G.S. Anitha, "Control Strategy to Generate PWM Signals with Stability Analysis for Dual Input Power Converter System," *Indonesian Journal of Electrical Engineering and Informatics (IJEI)*, vol. 7, no. 4, pp. 609-619, 2019. [[CrossRef](#)] [[Google Scholar](#)] [[Publisher Link](#)]
- [13] Feiyang Zhu, and Qiang Li, "Coupled Inductors with an Adaptive Coupling Coefficient for Multiphase Voltage Regulators," *IEEE Transactions on Power Electronics*, vol. 38, no. 1, pp. 739-749, 2023. [[CrossRef](#)] [[Google Scholar](#)] [[Publisher Link](#)]
- [14] Nagesh, L., C. V. Bhanuprakash, and Singh BK. "Design and Implementation of Triple Output Forward DC-DC Converter with Coupled Inductor as Post-regulator for Space Application." In *2020 International Conference on Smart Technologies in Computing, Electrical and Electronics (ICSTCEE)*, pp. 175-179. IEEE, 2020. [[CrossRef](#)] [[Google Scholar](#)] [[Publisher Link](#)]
- [15] Pramod Kumar Rampelli et al., "Multiple-Output Magnetic Feedback Forward Converter with Discrete PWM for Space Application," *2012 IEEE International Conference on Power Electronics, Drives and Energy Systems (PEDES)*, Bengaluru, India, pp. 1-6, 2012. [[CrossRef](#)] [[Google Scholar](#)] [[Publisher Link](#)]
- [16] Jennifer Ian G. Ligtao et al., "Implementation of On-Chip OVP, OCP and OTP Circuits for DC-DC Converter Design," *2018 IEEE 10th International Conference on Humanoid, Nanotechnology, Information Technology, Communication and Control, Environment and Management (HNICEM)*, Baguio City, Philippines, pp. 1-6, 2018. [[CrossRef](#)] [[Google Scholar](#)] [[Publisher Link](#)]
- [17] Aravind Bhat et al., "Multiple Output Forward DC-DC Converter with Mag-Amp Post Regulators and Voltage Feedforward Control for Space Application," *2016 Biennial International Conference on Power and Energy Systems: Towards Sustainable Energy (PESTSE)*, Bengaluru, India, pp. 1-6, 2016. [[CrossRef](#)] [[Google Scholar](#)] [[Publisher Link](#)]
- [18] Dharmraj V. Ghodke, and K. Muralikrishnan, "ZVZCS, Dual, Two-Transistor Forward DC-DC Converter with Peak Voltage of Vin/2, High Input and High-Power Application," *2002 IEEE 33rd Annual IEEE Power Electronics Specialists Conference. Proceedings (Cat. No. 02CH37289)*, Cairns, QLD, Australia, vol. 4, pp. 1853-1858, 2002. [[CrossRef](#)] [[Google Scholar](#)] [[Publisher Link](#)]
- [19] Kefas D. Coelho, and Ivo Barbi, "A Three-Level Double-Ended Forward Converter," *IEEE 34th Annual Conference on Power Electronics Specialist, 2003. PESC '03.*, Acapulco, Mexico, vol. 3, pp. 1396-1400, 2003. [[CrossRef](#)] [[Google Scholar](#)] [[Publisher Link](#)]
- [20] Sunil Kumar, and Apoorv, "Non-Cascading Structure for Wide Duty Cycle in Forward Converter," *2024 IEEE 3rd International Conference on Electrical Power and Energy Systems (ICEPES)*, Bhopal, India, pp. 1-5, 2024. [[CrossRef](#)] [[Google Scholar](#)] [[Publisher Link](#)]
- [21] Suresh Kumar Tummala, and Lenine Duraiswamy, "Switched Mode Power Supply: A Highly Efficient Low Noise Forward Converter Design Topology," *2022 IEEE 2nd International Conference on Sustainable Energy and Future Electric Transportation (SeFeT)*, Hyderabad, India, pp. 1-5, 2022. [[CrossRef](#)] [[Google Scholar](#)] [[Publisher Link](#)]
- [22] Srijana. R. Savanur et al., "Hardware Implementation of Forward Converter with Active Clamp Reset Technique," *2020 International Conference on Smart Technologies in Computing, Electrical and Electronics (ICSTCEE)*, Bengaluru, India, pp. 293-297, 2020. [[CrossRef](#)] [[Google Scholar](#)] [[Publisher Link](#)]

[23] Danamma M. Sangalad et al., "Design and Analysis of Dual Input SEPIC Converter for Renewable Energy Sources," *2015 International Conference on Emerging Research in Electronics, Computer Science and Technology (ICERECT)*, Mandya, India, pp. 358-363, 2015. [\[CrossRef\]](#) [\[Google Scholar\]](#) [\[Publisher Link\]](#)

[24] Daniel W. Hart, *Power Electronics*, vol. 166, New York: McGraw-Hill, 2011. [\[Google Scholar\]](#) [\[Publisher Link\]](#)